Biophysical Chemistry 159 (2011) 41–47

Contents lists available at ScienceDirect

Biophysical Chemistry

journal homepage: http://www.elsevier.com/locate/biophyschem

Conformational dynamics promote binding diversity of dynein light chain LC8☆

Afua Nyarko [a], Justin Hall [a], Andrea Hall [a], Michael Hare [a], Joachim Kremerskothen [b], Elisar Barbar [a,*]

[a] Department of Biochemistry and Biophysics, Oregon State University, Corvallis, OR 97331, United States
[b] Department of Molecular Nephrology, University Hospital Muenster, Muenster, Germany

ARTICLE INFO

Article history:
Received 1 April 2011
Received in revised form 1 May 2011
Accepted 1 May 2011
Available online 6 May 2011

Keywords:
Isothermal titration calorimetry
Backbone 15N relaxation
Binding diversity
Hub protein

ABSTRACT

A highly conserved and ubiquitous protein known as LC8 binds over twenty different partners, characteristic of a molecular hub (Barbar, 2008 *Biochemistry*, **47**, 503–508). Structural studies of LC8 complexes with binding partners having diverse recognition sequences show that the same binding groove of LC8 accommodates the various binding motifs. Here we use thermodynamics and dynamics measurements of LC8 complexes to group LC8 binding partners in two categories: those whose binding is enthalpically driven and those that are entropically favored. Peptides that are enthalpically driven completely silence the millisecond–microsecond relaxation signal, suggesting a significant rigidifying of the binding groove, while peptides in the entropically favored group exhibit the same conformational dynamics as the free protein, suggesting that the peptide sits loosely in the binding groove and so retains flexibility of the groove, and presumably of the bound peptide. The inherent disorder in the LC8 binding groove and in LC8 binding partners allows both types of binding, accounts for the lack of a conserved recognition consensus motif and underlies the binding specificity and broad selectivity observed in LC8 binding.

1. Introduction

LC8 is a highly conserved dimeric protein that was originally identified as a dynein light chain [1], later as a light chain of myosin Va [2], and eventually as a component of various complexes unrelated to motor proteins [3]. LC8 directly interacts with dynein intermediate chain, IC [4,5], neuronal nitric oxide synthase, nNOS [6], the proapoptotic Bcl2 interacting mediator, Bim [7], the Bcl2 modifying factor, Bmf [8], the transcription factor Swallow, Swa [9], the tumor suppressor Kibra [10], the p21-activated protein kinase (Pak1) [11], and many others [3] (Fig. 1). LC8 is a homodimer with a cross over β-strand from each protomer forming two identical grooves at the dimer interface [12]. Most known LC8 binding partners have either a KXTQT or a less common GIQVD binding motif [13]. A recently identified recognition sequence in Pak1 does not belong to either motif [11]. Crystal and NMR structures of LC8 bound to consensus sequence peptides are essentially similar and show that the KXTQT (Bim, IC and Swa), the GIQVD (nNOS), and the DVATSP (Pak1) binding sequences adopt a sixth β strand adjacent to β3 at the LC8 dimer interface [11,12,14,15] (Fig. 2).

The unusually wide range of biologically important ligands that bind at the same LC8 groove raises a number of intriguing questions, among the most important of which are: What is the biological function(s) of LC8? What biophysical factors account for its remarkable binding diversity? To answer the first question, we have proposed that the biological function of LC8 is to act as a molecular hub promoting dimerization and subsequent assembly of intrinsically disordered proteins in diverse systems [3,16]. The second question, the molecular biophysics underlying its binding diversity, is examined here.

Comparison of the crystal structures of various LC8 complexes to the apo protein structure shows subtle differences at the binding interface. Peptides with the GIQVD motif expand the binding pocket by about 2 Å, while those with the KXTQT motif expand the binding pocket by about 1 Å [17]. The expansion is caused by sliding of the main chain of one subunit relative to the other. This somewhat unusual expansion of the binding pocket allows peptides with different volumes to share the same binding site. While the crystal structures of LC8 with and without bound ligand give insight into how the geometry of the pocket may accommodate different sized peptide partners, it remains unclear what molecular processes drive molecular recognition. A glutamine residue found in most sequences (position 8 in Fig. 3a) was proposed to be essential for recognition and stability of the complex as it is involved in several interactions with both protomers (Fig. 3b) [15]. However, many sequences do not contain a glutamine residue but yet still bind with remarkable specificity.

^{15}N NMR relaxation studies analyzed using the model-free approach show that the target peptide-binding region [18] and other regions of the protein [19] experience microsecond-to-millisecond time scale conformational fluctuations. In LC8 bound to short peptides of Swallow [19], and Bim [18], both containing the KXTQT motif, the conformational heterogeneity apparent in the LC8 dimer is lost in LC8/Swa and LC8/Bim, indicating the absence of internal mobility on the millisecond-to-microsecond time scale. Interestingly, in LC8

☆ This work is supported by NSF grant MCB 0818896 to E.B. and a predoctoral AHA fellowship 09PRE2250819 to J.H.

* Corresponding author. Tel.: +1 541 737 4143; fax: +1 541 737 0481.
E-mail address: barbare@science.oregonstate.edu (E. Barbar).

0301-4622/$ – see front matter © 2011 Elsevier B.V. All rights reserved.
doi:10.1016/j.bpc.2011.05.001

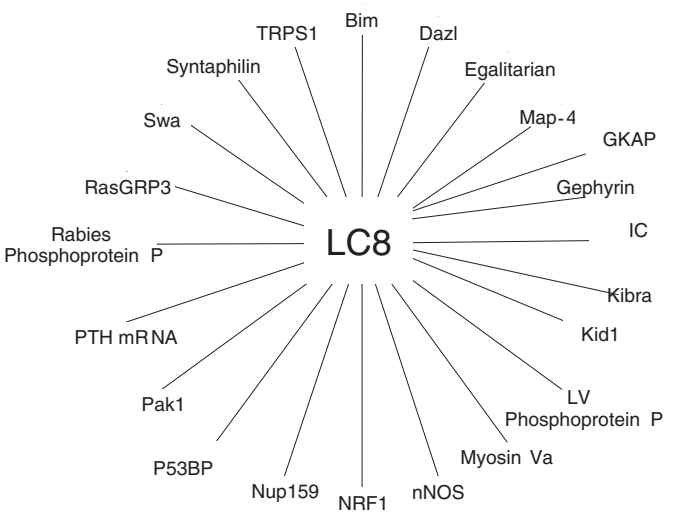

Fig. 1. LC8 is a molecular hub. Binding partners are dynein intermediate chain, IC; the tumor suppressor Kibra; a zinc finger transcription factor expressed in response to renal injury Kid-1 [13]; Lyssavirus phosphoprotein P[32]; Myosin Va; neuronal nitric oxide synthase, nNOS; transcription factor NRF1 [33]; yeast nuclear pore complex protein 159, Nup159 [34]; p53 binding protein 1, p53 BP [35]; p21-activated kinase-1, Pak1 [36]; parathyroid hormone mRNA, PTH mRNA[37]; rabies virus phosphoprotein; an exchange factor for Ras-like small GTPases, RasGRP, whose interaction with LC8 is responsible for its subcellular localization [38]; Swallow protein, Swa; Syntaphilin [39]; a repressor of GATA-regulated genes, TRPS1, [40] whose interaction with LC8 in the cell nucleus results in suppressing its transcriptional repression activity; Bim, a proapoptotic Bcl2 family protein [7] whose interaction with LC8 promotes apoptosis [36]; Dazl [41]; Egalitarian[42]; MAP-4, MT-associated protein 4 [13]; GKAP, Guanylate kinase-associated protein neuronal scaffold whose interaction with LC8 is involved in trafficking of the postsynaptic density-95 complex [43]; and Gephyrin [44].

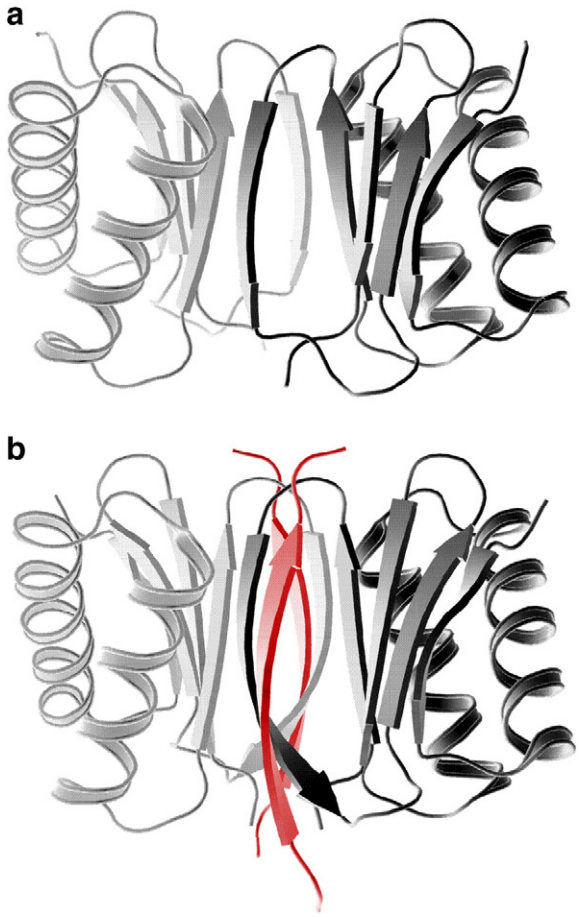

Fig. 2. All known LC8 partners bind as β-strands in the grooves at the LC8 homodimer interface. a) Structure of homodimeric apo-LC8 (the two chains of LC8 are colored black and gray), and b) the nNOS•LC8 complex (red•black/gray) show bound peptides are related by 2-fold symmetry parallel to the LC8 homodimer axis and bind equivalent LC8 residues. Figures were generated using Pymol [45] with pdb structures 3BRI (apo-LC8) [17], 1CMI (nNOS•LC8) [12].

bound to short peptides of IC [19], which also contains the KXTQT motif, conformational heterogeneity is retained in LC8/IC complex suggesting that the degree of ordering upon binding is ligand dependent [19]. Binding energetics determined from isothermal titration calorimetry show that for LC8/Swa and LC8/Bim complexes, binding is enthalpically favored, while for LC8/IC complex, binding is entropically favored [19].

To determine whether changes in dynamics and conformational entropy are dependent on the recognition sequence, we perform heteronuclear NMR relaxation studies on LC8 bound to a peptide with the GIQVD motif, and rigorous thermodynamic analysis on LC8 bound to several other peptides with diverse sequences. We group binding partners in two categories regardless of their recognition sequences: those with enthalpically driven binding, and those with entropically favored binding. Each group reveals relaxation patterns that are independent of residue specificity suggesting a larger role for conformational entropy in driving LC8 recognition to its binding partners.

2. Methods

2.1. Protein preparation

LC8 was prepared following methods described earlier [20]. Synthetic peptides (Biosynthesis Inc., Lewisville, TX) were purified following methods previously described [19].

2.2. Isothermal titration calorimetry

Binding experiments were carried out using a VP-ITC micro calorimeter from MicroCal (Northampton, MA). Data were processed using the manufacturer's supplied software package, Origin 7.0 (OriginLab Corp., Northampton, MA). Heats of dilution, determined from titrating protein into buffer were subtracted from the binding data prior to fitting. Data were well fit using single-site binding model: **A** + **B** → **AB**, where **A** refers to a single peptide chain in the syringe and **B** refers to a single protein chain in the cell. For all experiments the "c value" ($c = [\text{protein}]_{\text{sample cell}} \times K_d^{-1}$) was within the 5 to 500 range required for reliable determination of association constants using a syringe/cell concentration of 0.5/0.03 mM and a stir rate of 351 rpm. The concentration of LC8 was determined using the sequence-based calculated extinction coefficient of 13370 $M^{-1}\,cm^{-1}$, while the peptide concentrations were determined from their dry weights. Thermodynamic association parameters for LC8 binding to Bim, IC, nNOS and Swa were measured in 50 mM sodium phosphate, 50 mM sodium citrate, 50 mM sodium chloride, 1 mM sodium azide, pH 5.5 at 30 °C and in the temperature range of 5 to 35 °C. For binding to Kib1 and Kib2 in 50 mM sodium phosphate buffer, pH 7.5 and 25 °C, peptide/LC8 concentrations of 0.3/0.02 mM for Kib1 and 0.55/0.04 mM Kib2 were used. Each interaction gave a binding stoichiometry of 1. Data reported are an average of two experiments performed under similar conditions.

2.3. NMR spectroscopy

NMR spectra for the nNOS•LC8 complex were collected and analyzed following methods previously described to allow direct

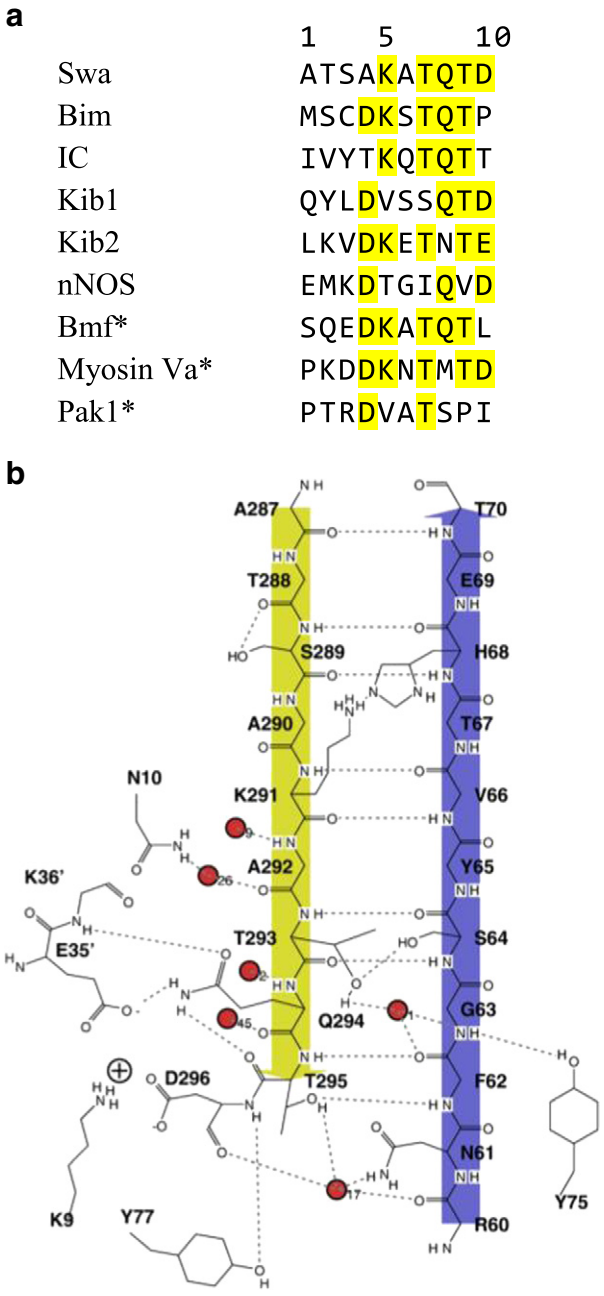

Fig. 3. (a) Recognition sequences of LC8 binding partners showing residues in direct contact with LC8. For most of the peptides, the consensus binding motif is preceded by an aspartate. The asterisks denote peptides whose binding was reported in Ref. [23]. (b) A schematic of specific contacts between Swa peptide (yellow) and LC8 (subunit 1 blue, subunit 2 cyan). Fig. 3b is adapted from [15].

comparison to LC8 in complex with other peptides [19]. Briefly, nNOS•LC8 samples were prepared with 5 mM unlabelled nNOS and 1 mM ^{15}N-labeled LC8. Experiments were collected at 25 °C and ^{1}H chemical shifts were referenced from an internal DSS signal at zero ppm. HNCA and CBCACONH experiments for nNOS•LC8 backbone assignments were performed with 1024 (H), 64 (C) and 20 (N) points. R_1, R_2 and steady state heteronuclear NOE spectra were recorded using the pulse sequence described by Farrow et al. [21], processed with NMRPipe and analyzed with Burrow-Owl [22]. R_1 and R_2 data were fit using CurveFit v1.3 (http://biochemistry.hs.columbia.edu/labs/palmer/software/curvefit.html).

Relaxation parameters were analyzed with the extended Lipari–Szabo formalism as described in Ref. [19]. The global tumbling correlation time (τ_m) was calculated from the R_2/R_1 ratio for qualifying residues. Correlation times and rotational diffusion parameters were determined using Gaussian Monte Carlo simulations. A model for internal motions was rejected if the experimental χ^2 value was higher than the simulated χ^2 value at a 90% confidence level. For anisotropic analyses, pdb code 1CMI [12] was used to fit nNOS•LC8 data.

3. Results and discussion

3.1. Thermodynamics of LC8 binding to peptide partners

Isothermal titration calorimetry was used to determine the binding energetics of LC8 with 16–20 amino acid peptides from several partners with diverse recognition sequences (Fig. 3). All share a common recognition groove on LC8. While there are no high resolution structures for Kib1 and Kib2 (peptides from the tumor suppressor Kibra), competition experiments do not reveal alternate binding sites other than the consensus groove (data not shown).

Representative binding isotherms for LC8 with nNOS, Kib1, and Kib2, are shown in Fig. 4. Binding isotherms for LC8 with Swa, IC, and Bim at 30 °C were reported earlier [19]. Association parameters (ΔG°, ΔH°, -TΔS°) and the related heat capacity change (ΔCp) are given in Table 1. Interestingly, while these peptides bind LC8 with similar free binding energy (7.4–8.7 kcal/mol), they exhibit two different modes of binding. With Bim, Kib1 and Swa, binding is enthalpically favored with a change in enthalpy in the range of 10–12 kcal/mol (Fig. 5 and Table 1). In contrast, with Kib2, IC, and nNOS, binding is entropically favored with TΔS° in the range of 3–5 kcal/mol.

Binding data were collected in the temperature range of 5 °C to 35 °C. Fig. 6 shows representative binding isotherms for Swa, Bim, nNOS and IC at 10 °C. Binding of Swa and Bim is enthalpically driven in this temperature range, while binding of nNOS and IC is entropically driven. The binding of the four peptides is associated with a similar ΔCp value of -0.25 ± 0.04 kcal·mol^{-1}·K^{-1} (Table 1). Because a change in heat capacity reflects burial of nonpolar surface, the implication of similar ΔCp is that the four ligands bury a similar surface area. In the crystal structure of apo-LC8, the exposed hydrophobic surface area arises primarily from β4 strand and corresponds to ~100 Å^2 [17]. In all four bound complexes, this area is completely buried, and a GIQVD motif peptide (nNOS) expands this surface by an additional 100 Å^2, while a KXTQT motif peptide (Swa, IC and Bim) expands this surface by 50 Å^2; the total surface in contact with the peptides is ~200 Å^2 and ~150 Å^2, respectively. The similar burial of exposed surface area for KXTQT motif peptides indicates that solvent entropy does not have a major contribution to the different thermodynamic signatures.

The binding of nNOS and three other peptides (Fig. 3a, asterisk) was reported recently by Nyitray and coworkers [23], and discussed here for comparison. Bmf binding is enthalpically driven, while myosin Va and Pak1 binding is entropically favored. In addition, Pak1 binding is considerably weaker than the rest. The pattern that emerges from comparison of all these data is that, contrary to what was suggested in Ref. [23], the consensus motif does not appear to determine the mode of binding as there are peptides containing the KXTQT motif that are either enthalpically (Bim, Bmf, Swa) or entropically (IC) favored.

3.2. Changes in LC8 dynamics upon binding are peptide dependent

^{15}N-backbone relaxation measurements (R_1, R_2 and steady state heteronuclear NOEs) were collected for nNOS•LC8 (Fig. 7) and analyzed using the model free approach. While the data are consistent with a well-folded isotropically tumbling protein, there is significant deviation from the simple tumbling model as some residues have effective local

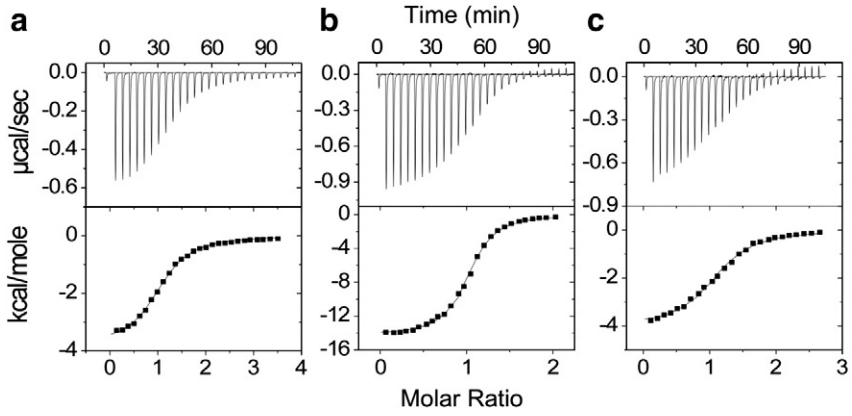

Fig. 4. Representative ITC thermograms (top panels) and binding isotherms (bottom panels) for LC8 binding with nNOS at 35 °C (a), Kib1 at 25 °C (b), and Kib2 at 25 °C (c).

correlation times (τe) that differ from the overall correlation time. These amide vectors also require large exchange broadening (Rex) values to reproduce the experimental relaxation data, indicating that they experience microsecond-to-millisecond time scale fluctuations, arising from greater conformational diversity.

Interpretation of the relaxation data using the model-free approach provides insight into how ligand binding influences the amplitudes and time scales of backbone motions over a broad range of time scales. Differences in order parameters (S^2) values imply changes on the picosecond-nanosecond timescales, or motions that are faster than the overall correlation time of the protein, while differences in Rex terms indicate differences in millisecond to microsecond timescale motions [24].

Between apo and nNOS•LC8, and similar to apo and bound calmodulin [25], differences in backbone order parameters are too subtle to be significant as no substantial disorder to order transition accompany binding. Interesting changes, however, are reflected in the complexity of the models required to fit the relaxation data and in the number of residues with Rex terms (Fig. 7). With apo LC8, there are several residues across the protein with Rex terms>2 Hz indicating significant conformational heterogeneity [19] (Fig. 8). This pattern does not change with IC, while fewer residues with Rex terms are observed with nNOS. In contrast, with Swa, there are only two residues, and with Bim, there are no residues with Rex terms above 2 Hz [18]. Thus we conclude that the persistence of backbone heterogeneity in the bound form depends on the ligand. With Bim and Swa, there is clear rigidifying of motion, suggesting that these peptides bind and lock LC8 into a more restricted conformational ensemble. On the other hand, with IC and nNOS the conformational heterogeneity observed in apo-LC8 persists to a varying degree, suggesting that these peptides sit loosely (i.e. retain flexibility) in the pocket and therefore permit the retention of a broad ensemble of multiple pocket conformations.

Table 1
Thermodynamic association parameters for LC8 binding to peptides from diverse partners.[a]

Peptide	*Kd (μM)*	*ΔG° (kcal/mol)*	*ΔH° (kcal/mol)*	*-TΔS° (kcal/mol)*	*ΔCp[c] (kcal/mol/K)*
Bim	0.52 ± 0.03	−8.7 ± 1	−10.4 ± 0.1	1.7 ± 0.2	−0.29
Kib1[b]	0.45 ± 0.03	−8.53 ± 0.08	−12.5 ± 1.7	4.0 ± 1.6	
Swa	0.62 ± 0.04	−8.6 ± 0.6	−10.65 ± 0.08	2.0 ± 0.1	−0.22
Kib2[b]	4.0 ± 0.5	−7.4 ± 0.1	−4.5 ± 0.5	−2.9 ± 0.6	
IC	3.0 ± 0.1	−7.8 ± 0.4	−4.00 ± 0.04	−3.8 ± 0.2	−0.26
nNOS	2.0 ± 0.1	−7.90 ± 0.04	−2.98 ± 0.04	−4.91 ± 0.05	−0.24

[a] Values are determined at 30 °C from one experiment with error estimation based on data deviation from the theoretical best fit.
[b] Values are determined at 25 °C from the average of two experiments with error estimation from standard deviation between experimental repeats.
[c] Values are determined from ΔH temperature dependence in the 10–35 °C range. Data for Kib1 and Kib2 were only collected at 25 °C.

3.3. Sequence specificity and entropy–enthalpy compensation

In the crystal structures of LC8 complexes, the backbone β-sheet interaction between β3 of LC8 and residue 1–9 of the partner recognition sequence (Fig. 3) aligns the first residue of the partner sequences with Thr 70 of LC8 and aligns residue 9 with Phe 62 of LC8. The peptide numbering is based on residues at the interface and not on their position in the sequence. For details of the LC8-peptide interactions, we chose the 2.0 Å resolution structure of LC8-Swa complex (Fig. 3b) [17,26]. Residue 10 is not part of the β-strand but makes side chain contacts with Lys9 of LC8, an interaction that is presumably present in peptides where residue 10 is an Asp or a Glu, and thus is absent in Bim, IC, Bmf, and Pak1, which have Pro, Thr, Ile, and Leu residues, respectively. Residue 9 is a highly conserved Thr (Val in nNOS and Pro in Pak1) whose hydroxyl group makes a hydrogen bond with the LC8 backbone. Residue 8 is also a highly conserved Gln (Asn, Met, and Ser in Kib2, Myosin Va, and Pak1, respectively) whose Cβ and Cγ atoms make hydrophobic contacts with Ile34′, Glu35′, and Lys 36′ at the N-terminal end of helix 2′ of the other protomer. The Gln carboxamide is buried and makes hydrogen bonds with Lys 36′N and with Glu35′ carboxylate. Most of these contacts would also be present with Asn, and to a smaller extent with Met and Ser. The residue at position 5 is a highly conserved Lys (Val in Kib1 and Pak1, and Thr in nNOS). The positive charge of the amino group is stabilized by contacts with aromatic groups of His 68 and Phe 73 of LC8. The residue at position 4 is a highly conserved Asp (Ala in Swa, Thr in IC), and forms a hydrogen bond between its carboxyl group and the side-chain hydroxyl group of Thr 67 of LC8. This interaction is also present in Thr of IC but absent with Ala of Swa.

The interaction at position 10 is present in some peptides with entropically driven binding (nNOS, Kib2, MyosinVa) but missing in others (Pak1, IC). Likewise, this interaction is present in peptides with enthalpically driven binding (Swa and Kib1) but missing in others (Bim and Bmf). The interaction at position 9 is missing only with nNOS and Pak1 (both entropically driven). At position 8, all interactions are preserved but are perhaps weaker with Met and Ser of Myosin Va and Pak1 (both entropically driven). The structural correlations for changes at positions 5 and 4 are less straightforward as the change of Lys at position 5 to Val in Kib1 (enthalpically driven) and Pak1 (entropically driven) could be stabilizing, while the change to Thr in nNOS (entropically driven) may be neutral. At position 4, the change

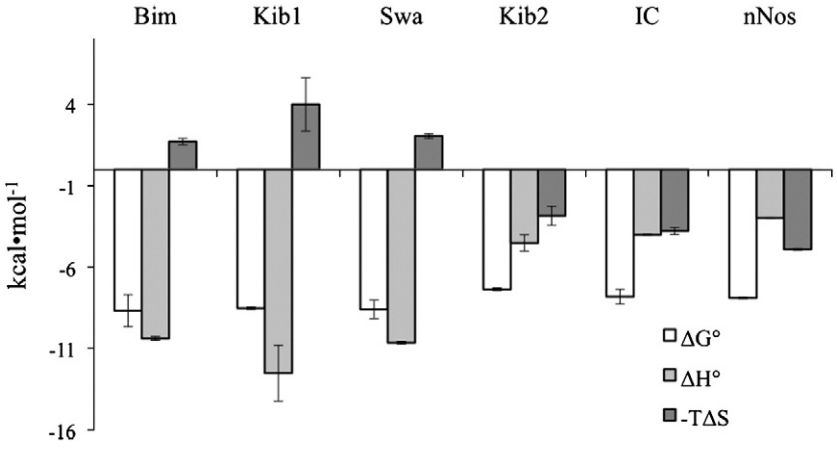

Fig. 5. Thermodynamics of binding for Bim, Kib1, Swa, Kib2, IC, and nNOS peptides with LC8. The changes in enthalpy (ΔH°), entropy (−TΔS°) and free energy of binding (ΔG°) are shown. Binding of Bim, Kib1, Swa is enthalpically driven (negative ΔH°) while binding of Kib2, IC, and nNOS is entropically favored (negative -TΔS°).

of Asp to Ala in Swa (enthalpically driven) could be entropically stabilizing; with Ala, there is no penalty for loss of conformational entropy of the side chain [27]. Thus, from this comparison two points are clear: Pak1 makes the least conserved interactions, which may explain its weaker binding [23], and some interactions are missing in entropically driven peptides. However, no pattern emerges from the sequences and crystal structures to specify either mode of binding.

3.4. Disorder to order transition in the binding partner

In crystal structures of LC8 bound to short peptide fragments, binding partners adopt a single beta strand at the LC8 dimer interface. There is, however, limited experimental characterization of the free peptides or of larger domains of the binding partners. One well-characterized binding partner is a 60-amino acid domain of IC that contains the LC8 consensus sequence [28]. NMR data show that the LC8 recognition sequence is fully disordered when free, consistent with prediction. Limited proteolysis experiments of the less characterized binding partner Swallow also show that the recognition sequence in Swallow is disordered [29]. Sequence analysis of various LC8 binding partners show that the recognition sequence is predicted to be primarily disordered and to contain some short beta strands [3]. Thus combining sequence prediction and experiments on representative binding partners suggest that the native disorder of the recognition sequence and the associated propensity for its formation of a short β-strand upon binding are common features among LC8 binding partners.

The beta strand observed in the crystal structure confirms a disorder to order transition in the recognition sequence. NMR data collected on ^{15}N labeled 60 amino acid segment of bound IC, however, show evidence for sampling of multiple conformations in the LC8-bound IC. Peaks in HSQC spectra disappear at the LC8 binding site during the titration due to exchange broadening [28]. This broadening could arise from exchange between free and bound (less likely as no peaks for the bound appear even at saturation) or from exchange between a beta strand structure and less ordered structure. The latter suggests that IC retains intermediate exchange motions consistent with conformational heterogeneity which likely contributes to a favorable entropy of binding. Dynamics on the IC recognition sequence inferred from exchange broadening are the only dynamics measurements on any LC8 recognition sequence as these studies are hampered by technical difficulties associated with NMR on large disordered proteins.

3.5. Conformational entropy and flexibility promote binding diversity and specificity

NMR backbone relaxation studies show that apo-LC8 samples a large distribution of multiple conformations and that ligand binding induces various degrees of rigidification in the millisecond to microsecond time scale. Upon Bim [18] and Swa [19] binding, there is apparently complete rigidification and restricted motion. However, with nNOS, reported in this work, there is some retained flexibility, while with IC, the remarkable conformational heterogeneity observed

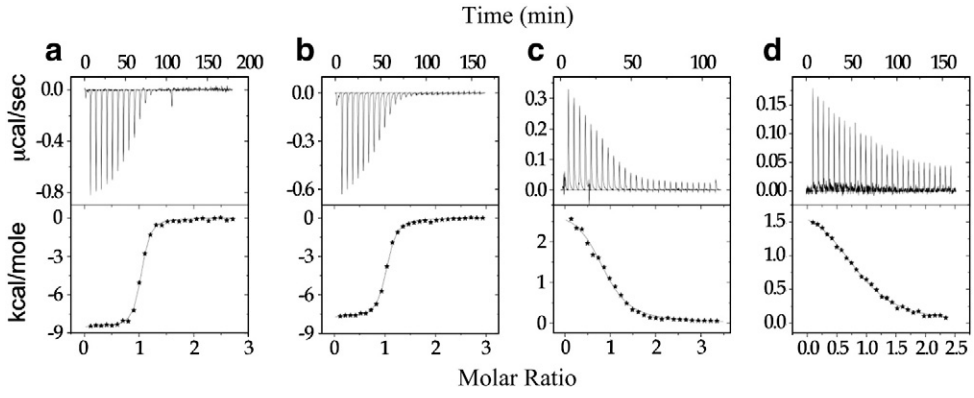

Fig. 6. Representative ITC thermograms (top panels) and binding isotherms (bottom panels) for LC8 binding with (a) Swa, (b) Bim, (c) nNOS, and (d) IC at 10 °C.

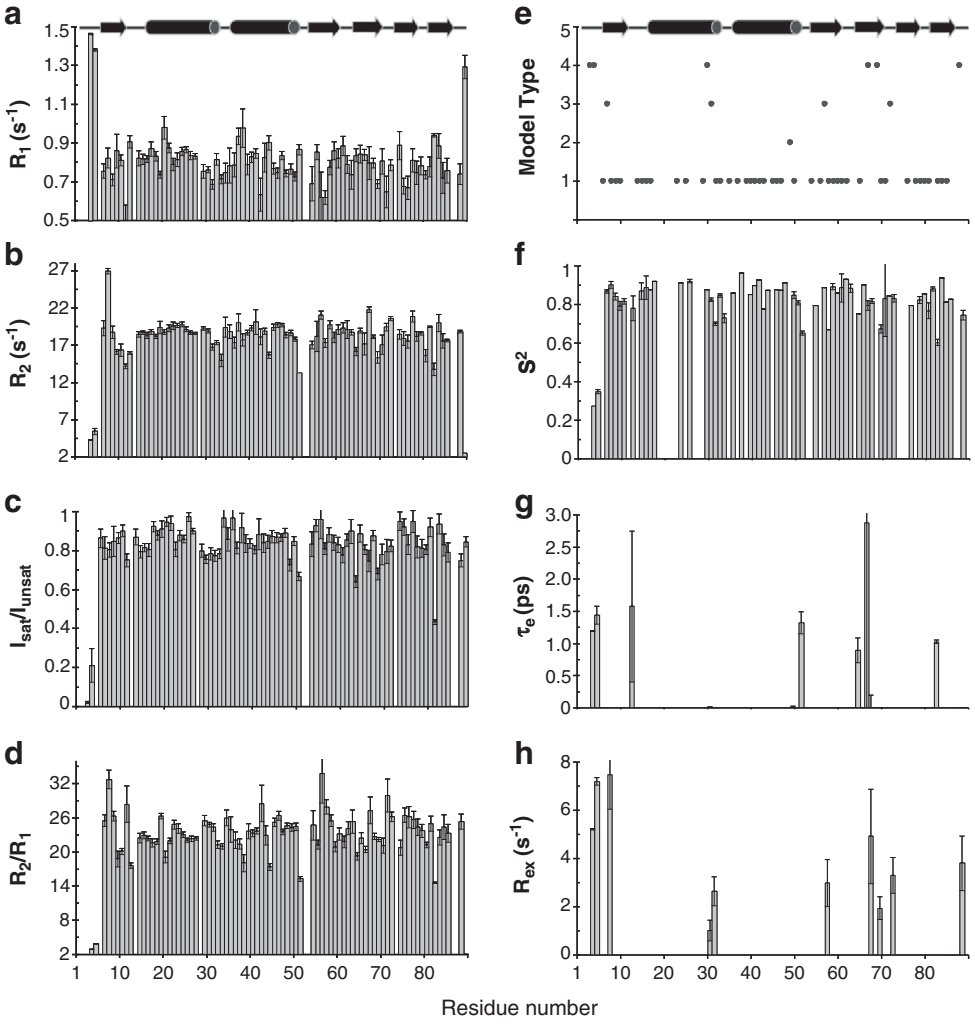

Fig. 7. LC8 retains τ_e and R_{ex} contributions to backbone heterogeneity after nNOS binding. Plots of a) R_1, b) R_2, c) steady-state ^1H, ^{15}N-NOE and d) R_2/R_1 dynamics data verses residue. Model free analysis with e) model type, f) S^2, g) τ_e and h) and R_{ex} parameters. Data for the nNOS•LC8 complex was collected at 25 °C, pH 5.5.

in apo-IC is fully retained [19]. Interestingly, the change in total entropy measured by ITC correlates with the NMR-determined changes in LC8 backbone heterogeneity indicating that retained conformational heterogeneity of LC8 contributes to the favorable entropy of binding and selects for partners that lack consensus enthalpic interactions.

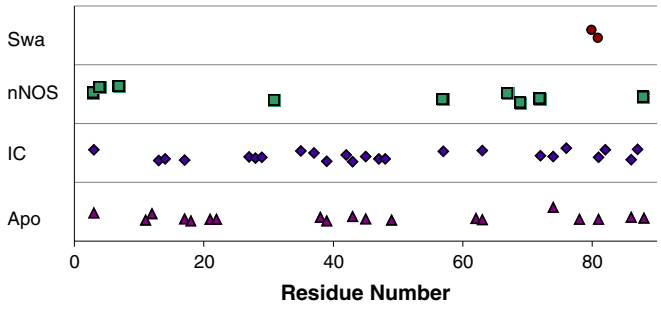

Fig. 8. Comparison of R_{ex} of apo and peptide-bound forms of LC8. The number of residues with R_{ex} terms >2 Hz is shown for apo-LC8 (▲), and LC8 bound to IC (♦), nNOS (■), Swa (●). While several residues in apo-LC8 and LC8/IC have R_{ex} values >2 Hz, only 9 residues and 2 residues with R_{ex} values >2 Hz are observed for LC8/nNos and LC8/Swa, respectively. None is observed with LC8/Bim.

Dynamical properties of the peptide would also contribute to the total entropy of the system. The natively disordered binding partners sample a large ensemble of conformations with some propensity for a beta strand structure, which when bound to LC8 as in the case of IC, retains considerable conformational heterogeneity. The loose insertion of IC in the LC8 binding pocket allows both the LC8 groove and IC to retain their flexibility and to contribute to favorable binding entropy. The differences in entropy of binding to various peptides therefore arise primarily from differences in conformational dynamics of LC8 and conformational dynamics of peptide partners, with minor contributions from solvent entropy.

There is a wealth of literature involving calmodulin that shows similar observations to what we report here with LC8, namely that conformational entropy regulates calmodulin's high affinity interactions and that changes in dynamics correlate with differences in thermodynamics of binding [30]. Calmodulin, like LC8, is a molecular hub that binds a large number of primarily disordered partners and has a flexible binding groove. Calmodulin is unusually dynamic on a picosecond–nanosecond timescale at the side chain level but not at the backbone level, and undergoes significant reorganization of side chain dynamics upon binding. Based on detailed quantitative side-chains relaxation measurements, Wand and coworkers show that the conformational entropy of calmodulin is linearly correlated with the total binding entropy and that changes in the conformational

entropy of calmodulin are a significant component of the energetic of binding [31].

In conclusion, we propose that LC8 fits a category of hub proteins that have evolved to sample multiple conformations to broaden their selectivity to diverse partners, and that the dynamical properties retained by the peptide and by the LC8 pocket after binding compensate for lack of sequence specificity and loss of otherwise crucial conserved interactions.

References

[1] S.M. King, E. Barbarese, J.F. Dillman, R.S. PatelKing, J.H. Carson, K.K. Pfister, Brain cytoplasmic and flagellar outer arm dyneins share a highly conserved M(r) 8000 light chain, The Journal of Biological Chemistry 271 (1996) 19358–19366.

[2] Z. Hodi, A.L. Nemeth, L. Radnai, C. Hetenyi, K. Schlett, A. Bodor, A. Perczel, L. Nyitray, Alternatively spliced exon B of myosin Va is essential for binding the tail-associated light chain shared by dynein, Biochemistry 45 (2006) 12582–12595.

[3] E. Barbar, Dynein light chain LC8 is a dimerization hub essential in diverse protein networks, Biochemistry 47 (2008) 503–508.

[4] M. Makokha, M. Hare, M.G. Li, T. Hays, E. Barbar, Interactions of cytoplasmic dynein light chains Tctex-1 and LC8 with the intermediate chain IC74, Biochemistry 41 (2002) 4302–4311.

[5] K.W.H. Lo, S. Naisbitt, J.S. Fan, M. Sheng, M.J. Zhang, The 8-kDa dynein light chain binds to its targets via a conserved (K/R)XTQT motif, The Journal of Biological Chemistry 276 (2001) 14059–14066.

[6] S.R. Jaffrey, S.H. Snyder, PIN: an associated protein inhibitor of neuronal nitric oxide synthase, Science 274 (1996) 774–777.

[7] H. Puthalakath, D.C.S. Huang, L.A. O'Reilly, S.M. King, A. Strasser, The proapoptotic activity of the Bcl-2 family member Bim is regulated by interaction with the dynein motor complex, Molecular Cell 3 (1999) 287–296.

[8] H. Puthalakath, A. Villunger, L.A. O'Reilly, J.G. Beaumont, L. Coultas, R.E. Cheney, D.C.S. Huang, A. Strasser, Bmf: a proapoptotic BH3-only protein regulated by interaction with the myosin V actin motor complex, activated by anoikis, Science 293 (2001) 1829–1832.

[9] F. Schnorrer, K. Bohmann, C. Nusslein-Volhard, The molecular motor dynein is involved in targeting Swallow and bicoid RNA to the anterior pole of Drosophila oocytes, Nature Cell Biology 2 (2000) 185–190.

[10] S.K. Rayala, P. den Hollander, B. Manavathi, A.H. Talukder, C. Song, S. Peng, A. Barnekow, J. Kremerskothen, R. Kumar, Essential role of KIBRA in co-activator function of dynein light chain 1 in mammalian cells, The Journal of Biological Chemistry 281 (2006) 19092–19099.

[11] C.M. Lightcap, S. Sun, J.D. Lear, U. Rodeck, T. Polenova, J.C. Williams, Biochemical and structural characterization of the Pak1-LC8 interaction, The Journal of Biological Chemistry 283 (2008) 27314–27324.

[12] J. Liang, S.R. Jaffrey, W. Guo, S.H. Snyder, J. Clardy, Structure of the PIN/LC8 dimer with a bound peptide, Nature Structural Biology 6 (1999) 735–740.

[13] I. Rodriguez-Crespo, B. Yelamos, F. Roncal, J.P. Albar, P.R. Ortiz de Montellano, F. Gavilanes, Identification of novel cellular proteins that bind to the LC8 dynein light chain using a pepscan technique, FEBS Letters 503 (2001) 135–141.

[14] J.S. Fan, Q. Zhang, H. Tochio, M. Li, M.J. Zhang, Structural basis of diverse sequence-dependent target recognition by the 8 kDa dynein light chain, Journal of Molecular Biology 306 (2001) 97–108.

[15] G. Benison, P.A. Karplus, E. Barbar, Structure and dynamics of LC8 complexes with KXTQT-motif peptides: swallow and dynein intermediate chain compete for a common site, Journal of Molecular Biology 371 (2007) 457–468.

[16] A. Nyarko, E. Barbar, Light chain-dependent self-association of dynein intermediate chain, The Journal of Biological Chemistry 286 (2011) 1556–1566.

[17] G. Benison, P.A. Karplus, E. Barbar, The interplay of ligand binding and quaternary structure in the diverse interactions of dynein light chain LC8, Journal of Molecular Biology 384 (2008) 954–966.

[18] J.S. Fan, Q. Zhang, H. Tochio, M. Zhang, Backbone dynamics of the 8 kDa dynein light chain dimer reveals molecular basis of the protein's functional diversity, Journal of Biomolecular NMR 23 (2002) 103–114.

[19] J. Hall, A. Hall, N. Pursifull, E. Barbar, Differences in dynamic structure of LC8 monomer, dimer, and dimer-peptide complexes, Biochemistry 47 (2008) 11940–11952.

[20] M. Makokha, Y.J. Huang, G. Montelione, A.S. Edison, E. Barbar, The solution structure of the pH induced monomer of dynein light chain from drosophila, Protein Science 13 (2004) 727–734.

[21] N.A. Farrow, O. Zhang, J.D. Forman-Kay, L.E. Kay, A heteronuclear correlation experiment for simultaneous determination of 15N longitudinal decay and chemical exchange rates of systems in slow equilibrium, Journal of Biomolecular NMR 4 (1994) 727–734.

[22] G. Benison, D.S. Berkholz, E. Barbar, Protein assignments without peak lists using higher-order spectra, Journal of Magnetic Resonance 189 (2007) 173–181.

[23] L. Radnai, P. Rapali, Z. Hodi, D. Suveges, T. Molnar, B. Kiss, B. Becsi, F. Erdodi, L. Buday, J. Kardos, M. Kovacs, L. Nyitray, Affinity, avidity, and kinetics of target sequence binding to LC8 dynein light chain isoforms, The Journal of Biological Chemistry 285 (2010) 38649–38657.

[24] A. Eletsky, A. Kienhofer, D. Hilvert, K. Pervushin, Investigation of ligand binding and protein dynamics in *Bacillus subtilis* chorismate mutase by transverse relaxation optimized spectroscopy-nuclear magnetic resonance, Biochemistry 44 (2005) 6788–6799.

[25] K.K. Frederick, J.K. Kranz, A.J. Wand, Characterization of the backbone and side chain dynamics of the CaM-CaMKIp complex reveals microscopic contributions to protein conformational entropy, Biochemistry 45 (2006) 9841–9848.

[26] G. Benison, P.A. Karplus, E. Barbar, Structure and dynamics of LC8 complexes with KXTQT-motif peptides: swallow and dynein intermediate chain compete for a common site, Journal of Molecular Biology 371 (2007) 457–468.

[27] M. Blaber, W.A. Baase, N. Gassner, B.W. Matthews, Alanine scanning mutagenesis of the alpha-helix 115–123 of phage T4 lysozyme: effects on structure, stability and the binding of solvent, Journal of Molecular Biology 246 (1995) 317–330.

[28] G. Benison, A. Nyarko, E. Barbar, Heteronuclear NMR identifies a nascent helix in intrinsically disordered dynein intermediate chain: implications for folding and dimerization, Journal of Molecular Biology 362 (2006) 1082–1093.

[29] L. Wang, M. Hare, T.S. Hays, E. Barbar, Dynein light chain LC8 promotes assembly of the coiled-coil domain of swallow protein, Biochemistry 43 (2004) 4611–4620.

[30] K.K. Frederick, M.S. Marlow, K.G. Valentine, A.J. Wand, Conformational entropy in molecular recognition by proteins, Nature 448 (2007) 325–329.

[31] M.S. Marlow, J. Dogan, K.K. Frederick, K.G. Valentine, A.J. Wand, The role of conformational entropy in molecular recognition by calmodulin, Nature Chemical Biology 6 (2010) 352–358.

[32] Y. Jacob, H. Badrane, P.E. Ceccaldi, N. Tordo, Cytoplasmic dynein LC8 interacts with lyssavirus phosphoprotein, Journal of Virology 74 (2000) 10217–10222.

[33] R.P. Herzig, U. Andersson, R.C. Scarpulla, Dynein light chain interacts with NRF-1 and EWG, structurally and functionally related transcription factors from humans and drosophila, Journal of Cell Science 113 (Pt 23) (2000) 4263–4273.

[34] P. Stelter, R. Kunze, D. Flemming, D. Hopfner, M. Diepholz, P. Philippsen, B. Bottcher, E. Hurt, Molecular basis for the functional interaction of dynein light chain with the nuclear-pore complex, Nature Cell Biology 9 (2007) 788–796.

[35] K.W. Lo, H.M. Kan, L.N. Chan, W.G. Xu, K.P. Wang, Z. Wu, M. Sheng, M. Zhang, The 8-kDa dynein light chain binds to p53-binding protein 1 and mediates DNA damage-induced p53 nuclear accumulation, The Journal of Biological Chemistry 280 (2005) 8172–8179.

[36] R.K. Vadlamudi, R. Bagheri-Yarmand, Z. Yang, S. Balasenthil, D. Nguyen, A.A. Sahin, P. den Hollander, R. Kumar, Dynein light chain 1, a p21-activated kinase 1-interacting substrate, promotes cancerous phenotypes, Cancer Cell 5 (2004) 575–585.

[37] E. Epstein, A. Sela-Brown, I. Ringel, R. Kilav, S.M. King, S.E. Benashski, J.K. Yisraeli, J. Silver, T. Naveh-Many, Dynein light chain binding to a 3 ′-untranslated sequence mediates parathyroid hormone mRNA association with microtubules, The Journal of Clinical Investigation 105 (2000) 505–512.

[38] S.M. Okamura, C.E. Oki-Idouchi, P.S. Lorenzo, The exchange factor and diacylglycerol receptor RasGRP3 interacts with dynein light chain 1 through its C-terminal domain, The Journal of Biological Chemistry 281 (2006) 36132–36139.

[39] Y.M. Chen, C. Gerwin, Z.H. Sheng, Dynein light chain LC8 regulates syntaphilin-mediated mitochondrial docking in axons, The Journal of Neuroscience : The Official Journal of the Society for Neuroscience 29 (2009) 9429–9438.

[40] F.J. Kaiser, K. Tavassoli, G.J. Van den Bemd, G.T.G. Chang, B. Horsthemke, T. Moroy, H.J. Ludecke, Nuclear interaction of the dynein light chain LC8a with the TRPS1 transcription factor suppresses the transcriptional repression activity of TRPS1, Human Molecular Genetics 12 (2003) 1349–1358.

[41] K.H. Lee, S. Lee, B. Kim, S. Chang, S.W. Kim, J.S. Paick, K. Rhee, Dazl can bind to dynein motor complex and may play a role in transport of specific mRNAs, The EMBO Journal 25 (2006) 4263–4270.

[42] C. Navarro, H. Puthalakath, J.M. Adams, A. Strasser, R. Lehmann, Egalitarian binds dynein light chain to establish oocyte polarity and maintain oocyte fate, Nature Cell Biology 6 (2004) 427–435.

[43] S. Naisbitt, J. Valtschanoff, D.W. Allison, C. Sala, E. Kim, A.M. Craig, R.J. Weinberg, M. Sheng, Interaction of the postsynaptic density-95/guanylate kinase domain-associated protein complex with a light chain of myosin- V and dynein, The Journal of Neuroscience 20 (2000) 4524–4534.

[44] J.C. Fuhrmann, S. Kins, P. Rostaing, O. El Far, J. Kirsch, M. Sheng, A. Triller, H. Betz, M. Kneussel, Gephyrin interacts with Dynein light chains 1 and 2, components of motor protein complexes, The Journal of Neuroscience : The Official Journal of the Society for Neuroscience 22 (2002) 5393–5402.

[45] W.L. DeLano, The PyMOL Molecular Graphics System, DeLano Scientific, San Carlos, CA, 2002.